eLIFE elifesciences.org

RESEARCH ARTICLE

Figures and figure supplements

Anterior CNS expansion driven by brain transcription factors

Jesús Rodriguez Curt *et al*

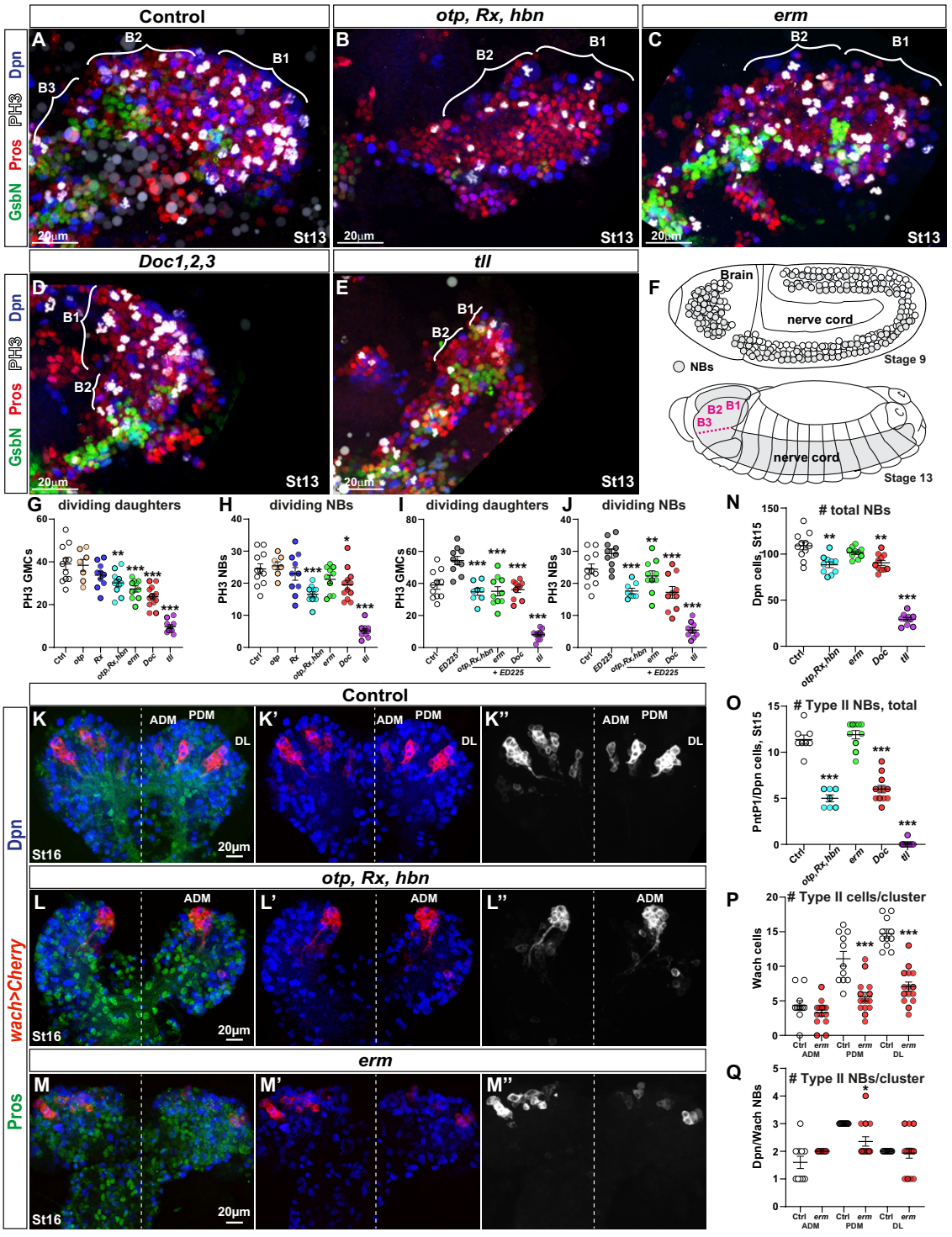

Figure 1. *Drosophila* brain TFs are required for proliferation and NB numbers. (**A-E**) Brain lobes at St13 of embryonic development, side views, anterior to the left. B1-B3 segments were delineated based on the expression of the segment-polarity marker GsbN, with a stripe of GsbN + cells marking the

Figure 1 continued on next page

Figure 1 continued

posterior edge of the each brain segment. PH3 labels mitotic cells. Dividing NBs are Dpn+/Pros asymmetric, while dividing daughter cells are Dpn-negative/Pros cytoplasmic. (**B-E**) Brain TF mutants show decreased proliferation and reduced brain size. (**F**) Schematic representation of the *Drosophila* CNS. During St8-11, the NBs are generated by delamination from the neuroectoderm, and there is a higher number of NBs in the B1 brain segment when compared to any posterior segment. By St13, NBs are undergoing lineage development, generating the brain and the nerve cord. (**G-J**) Quantification of dividing NBs and daughter cells in B1-B2, in control and brain gene mutants, with (**G-H**) or without PCD (**I-J**). Reduced proliferation is observed in both cases, that is when compared against wild type (G-H) or ED225 (I-J) (Student's t test; $*p \leq 0.05$, $**p \leq 0.01$, $***p \leq 0.001$; mean ± SEM; $n \geq 7$ embryos per genotype). (**K-K''**) In control, *wor-Gal4 ase-Gal80, UAS-20XCherry* (*wach*) labels the three Type II NB lineage clusters: Anterior Dorso Medial (ADM), Posterior Dorso Medial (PDM) and Dorso Lateral (DL). (**L-L''**) In *otp,Rx,hbn* triple mutants only one Type II cluster is observed. (**M-M''**) In *erm* mutants all three Type II clusters are observed, but are reduced in size. (**N**) Quantification of total NB number in B1-B2 segments in brain gene mutants. *Otp,Rx,hbn* and *Doc1,2,3* show significant but moderate decrease while *tll* shows a dramatic reduction of NBs in B1-B2 (Student's t test; $**p \leq 0.01$, $***p \leq 0.001$; mean ± SEM; $n \geq 10$ embryos per genotype). (**O**) Quantification of PntP1/Dpn positive cells in B1-B2 reveals a reduction in *Otp,Rx, hbn* and *Doc1,2,3* mutants, and a near total loss in *tll* mutants (Student's t test; $***p \leq 0.001$; mean ± SEM $n \geq 7$ embryos per genotype). (**P**) Quantification of cell numbers in Type II (*wach*) clusters in *erm* reveals reduced lineage size for PDM and DL clusters (Student's t test; $***p \leq 0.001$; mean ± SEM; $n \geq 11$ embryos per genotype). (**Q**) Quantification of NBs (Dpn+) in Type II (*wach*) clusters in control and *erm* mutants reveals a decrease in the PDM cluster (Student's t test; $*p \leq 0.05$; mean ± SEM; $n \geq 11$ embryos per genotype). All confocal images are maximum intensity projections of multiple focal planes.

DOI: https://doi.org/10.7554/eLife.45274.002

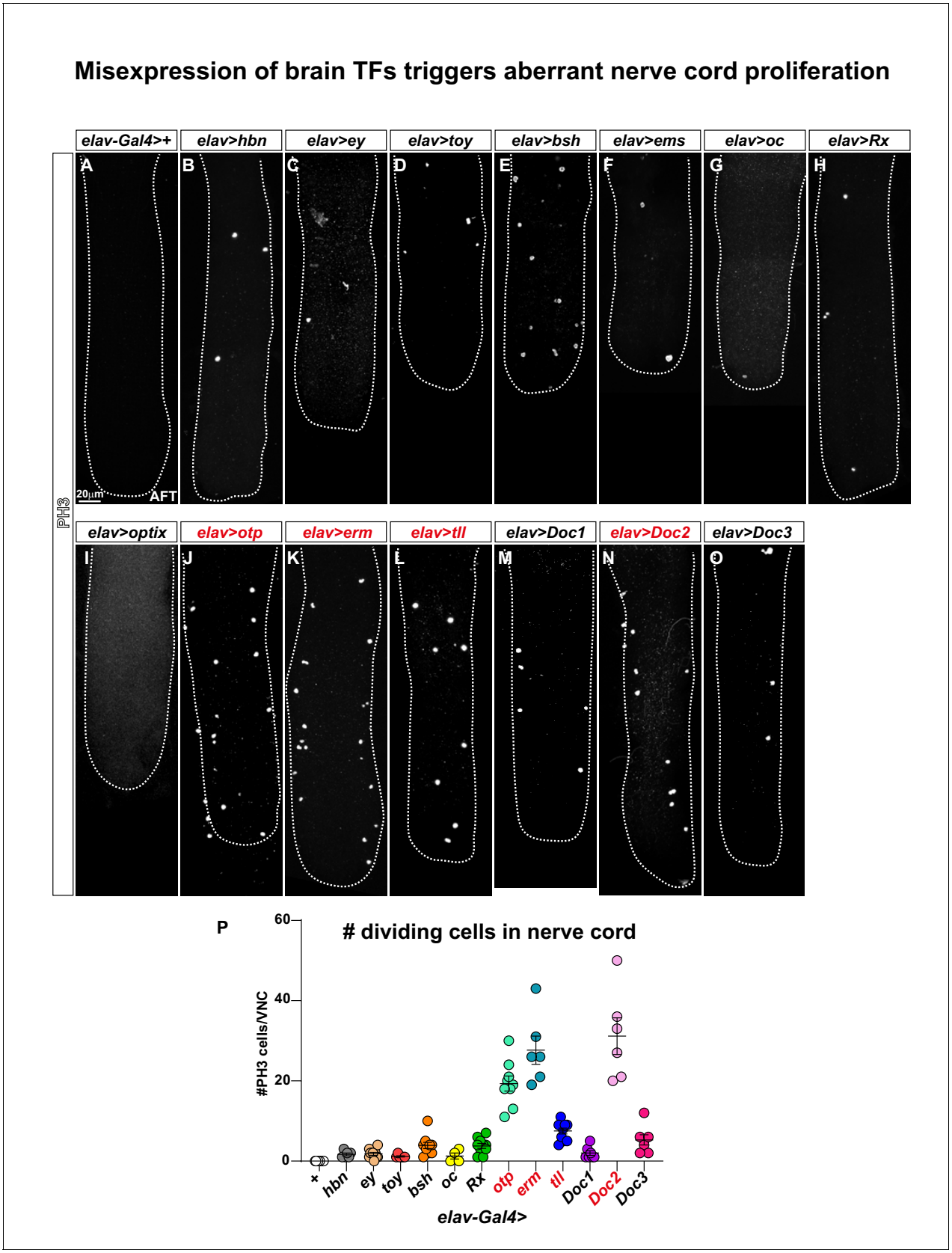

Figure 1—figure supplement 1. Misexpression of brain TFs triggers aberrant nerve cord proliferation. (**A**) Control (*elav-Gal4/+*) nerve cords show no mitotic cells (PH3) at stage AFT. (**B-O**) *elav-Gal4* driving different *UAS* brain gene transgenic lines results in different degrees of aberrant proliferation in

Figure 1—figure supplement 1 continued on next page

Figure 1—figure supplement 1 continued

the nerve cord. (**P**) Quantification of the number of dividing cells/nerve cord (PH3+) in control and *elav > UAS-* (mean ± SEM; n ≥ 4 embryos). *elav > ems* and *elav > optix* were not quantified, due to apparently minimal effects. Confocal images are maximum intensity projections of multiple focal planes.

DOI: https://doi.org/10.7554/eLife.45274.003

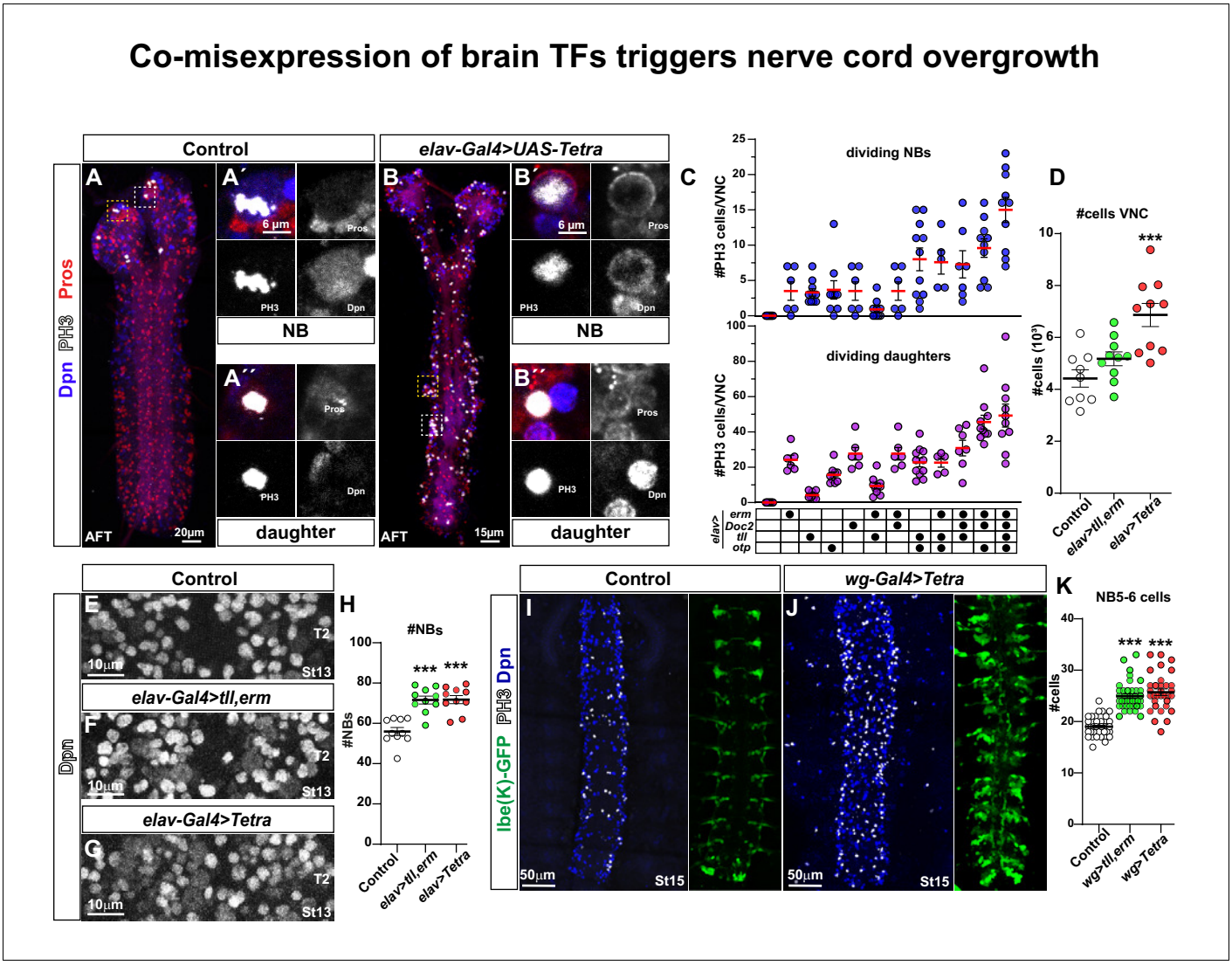

Figure 2. Co-misexpression of brain TFs triggers nerve cord overgrowth. (**A**) Control CNS (*elav-Gal4/+*) at AFT shows a few mitotic cells (PH3) in the brain lobes, but none in the nerve cord. (**A´**) Close-up of a mitotic NB and (**A´´**) a mitotic daughter cell. (**B**) Misexpression of four brain TFs, *elav-Gal4 > UAS* Tetra (*UAS-erm, UAS-Doc2, UAS-tll, UAS-otp*), triggers aberrant proliferation in the nerve cord at AFT. (**B´**) Close-up of a mitotic NB and (**B´´**) a mitotic daughter cell. (**C**) Quantitation of mitotic NBs and daughter cells per nerve cord (mean ± SEM; n ≥ 5 embryos per genotype) in control and different misexpression combinations of *UAS* transgenes. (D) Quantitation of total cell numbers in the nerve cord, in control (*elav-Gal4/+*), *elav > UAS tll,-erm* and *elav > UAS* Tetra (Student's t test; ***p≤0.001; mean ± SEM; n ≥ 9 embryos). (**E-G**) Dpn + cells (NBs) in control (*elav-Gal4/+*), *elav > UAS tll,-erm* and *elav > UAS* Tetra. (**H**) Quantification of NB numbers (Dpn + cells) at St13 in T2 (Student's t test; ***p≤0.001; mean ± SEM; n ≥ 10 embryos per genotype). (**I-J**) Nerve cords showing NBs (Dpn+) and the NB5-6 lineage (*lbe(K)-GFP*) at St15, in control (I; *wg-Gal4/+; lbe(K)-GFP/+*) and *wg-Gal4 > UAS* Tetra, showing an increased number of NBs (Dpn+), mitotic cells (PH3+) and an expanded NB5-6 lineage. (**K**) Quantitation of NB5-6 lineage cell numbers in the T2-T3 segments, at St15 (Student's t test; ***p≤0.001; mean ± SEM; n ≥ 10 embryos, n ≥ 32 lineages). All confocal images are maximum intensity projections of multiple focal planes. Zoomed in images are single optical sections.

DOI: https://doi.org/10.7554/eLife.45274.005

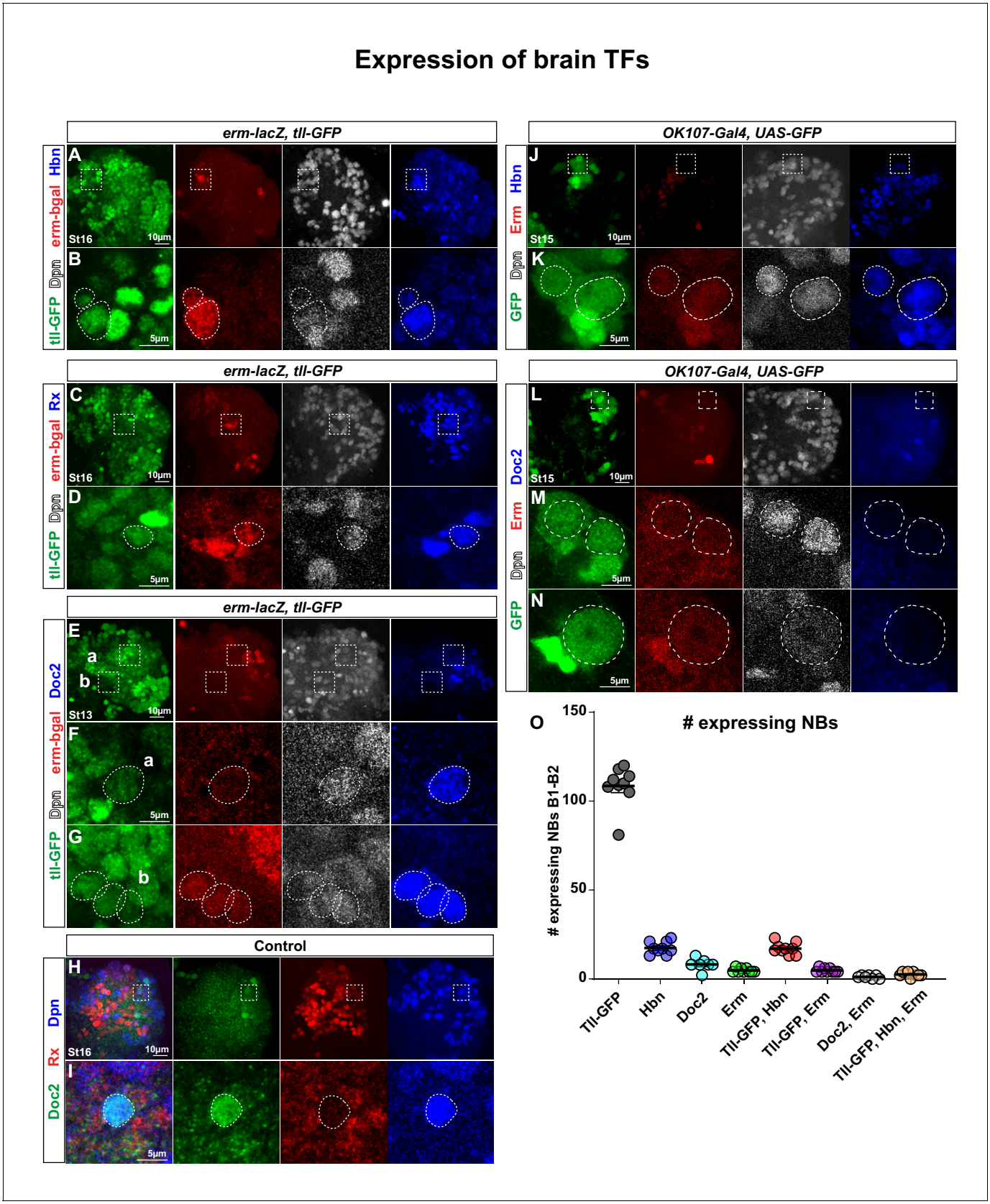

Figure 2—figure supplement 1. Expression of brain TFs in the developing embryo brain. (**A-B**) *tll-GFP* is expressed by many NBs throughout the brain, with *erm-lacZ* and Hbn overlapping with *tll-GFP* in a subset of NBs (dashed selections). (**C-D**) Rx is also expressed broadly in brain NBs, and overlaps

Figure 2—figure supplement 1 continued on next page

Figure 2—figure supplement 1 continued

with *tll-GFP* and *erm-lacZ*. (**E-F**) Doc2 expression is more restricted in the brain, but overlaps to some extent with *tll-GFP* and *erm-lacZ*. (**H-I**) Rx does not overlap with Doc2 in NBs. (**J-K**) MBNBs (marked by *OK107/UAS-GFP*) express Hbn but not Erm. (**L-N**) MBNBs express neither Doc2 nor Erm. (**O**) Quantification of the number of NBs in B1-B2 expressing each brain TF, and the number of NBs expressing overlapping combinations (mean ± SEM; n ≥ 7 embryos). Whole brain lobe panels are maximum intensity projections of multiple focal planes. Zoomed in panels are projections of 2–3 optical sections.

DOI: https://doi.org/10.7554/eLife.45274.006

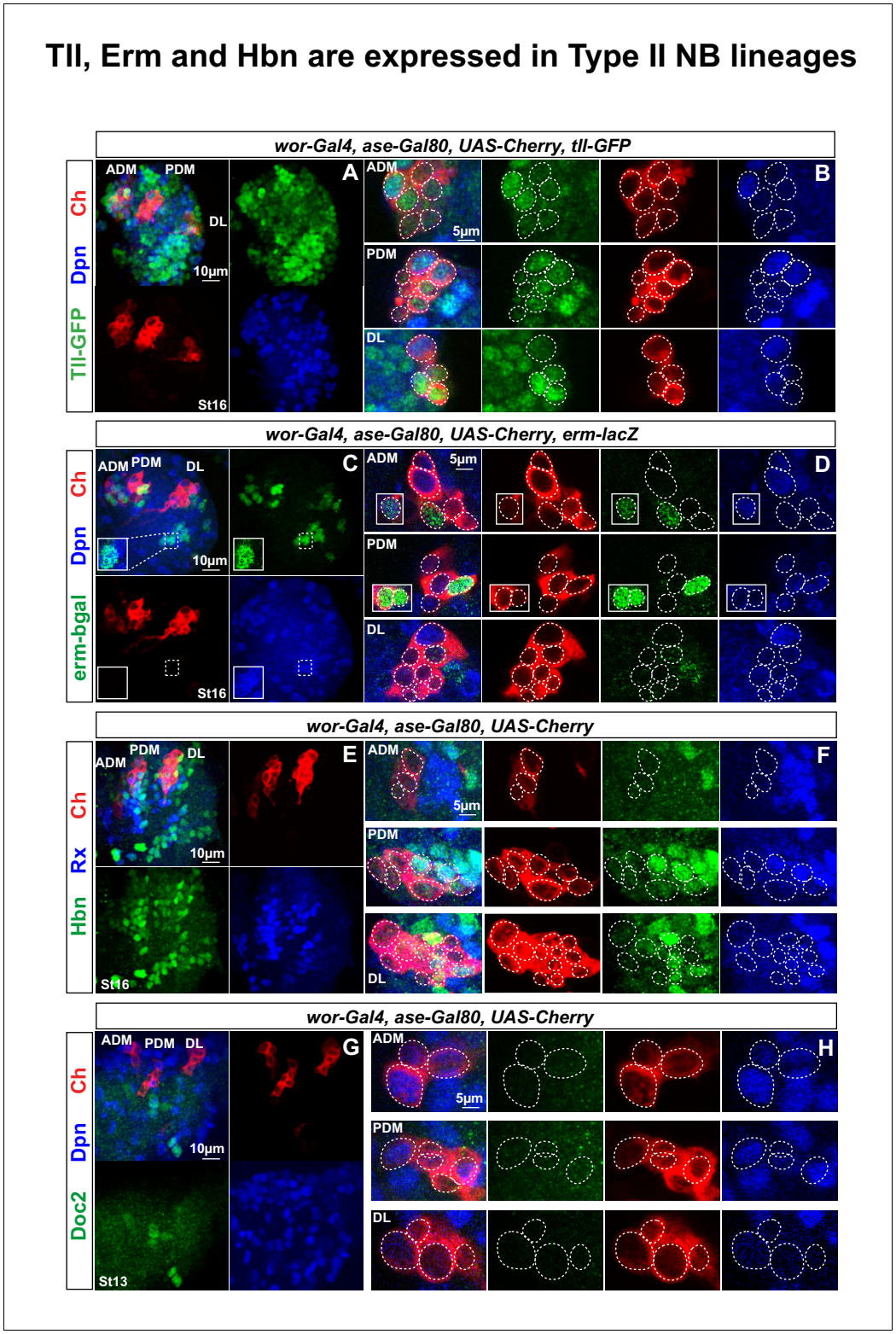

Figure 2—figure supplement 2. Expression of brain TFs in developing Type II NB lineages. (**A-H**) Expression of Dpn, Cherry (*wach*), *tll-GFP*, *erm-lacZ*, Rx, Hbn and Doc2, in the developing brain, at St16 (**A-F**) and St13 (**G-H**). (**D**) Inset panels correspond to different focal planes. (**A-B**) *tll-GFP* is expressed in all three Type II NB clusters (ADM, PDM and DL). (**C-D**) *erm-lacZ* is expressed in daughter cells in all three Type II NB clusters. (E-F) Rx and Hbn are expressed by the PDM and DL Type II lineages. (**G-H**) Doc2 is not expressed by any Type II NB lineage. Whole

Figure 2—figure supplement 2 continued on next page

Figure 2—figure supplement 2 continued

brain lobe panels are maximum intensity projections of multiple focal planes. Zoomed in panels are projections of 1–2 optical sections. .

DOI: https://doi.org/10.7554/eLife.45274.007

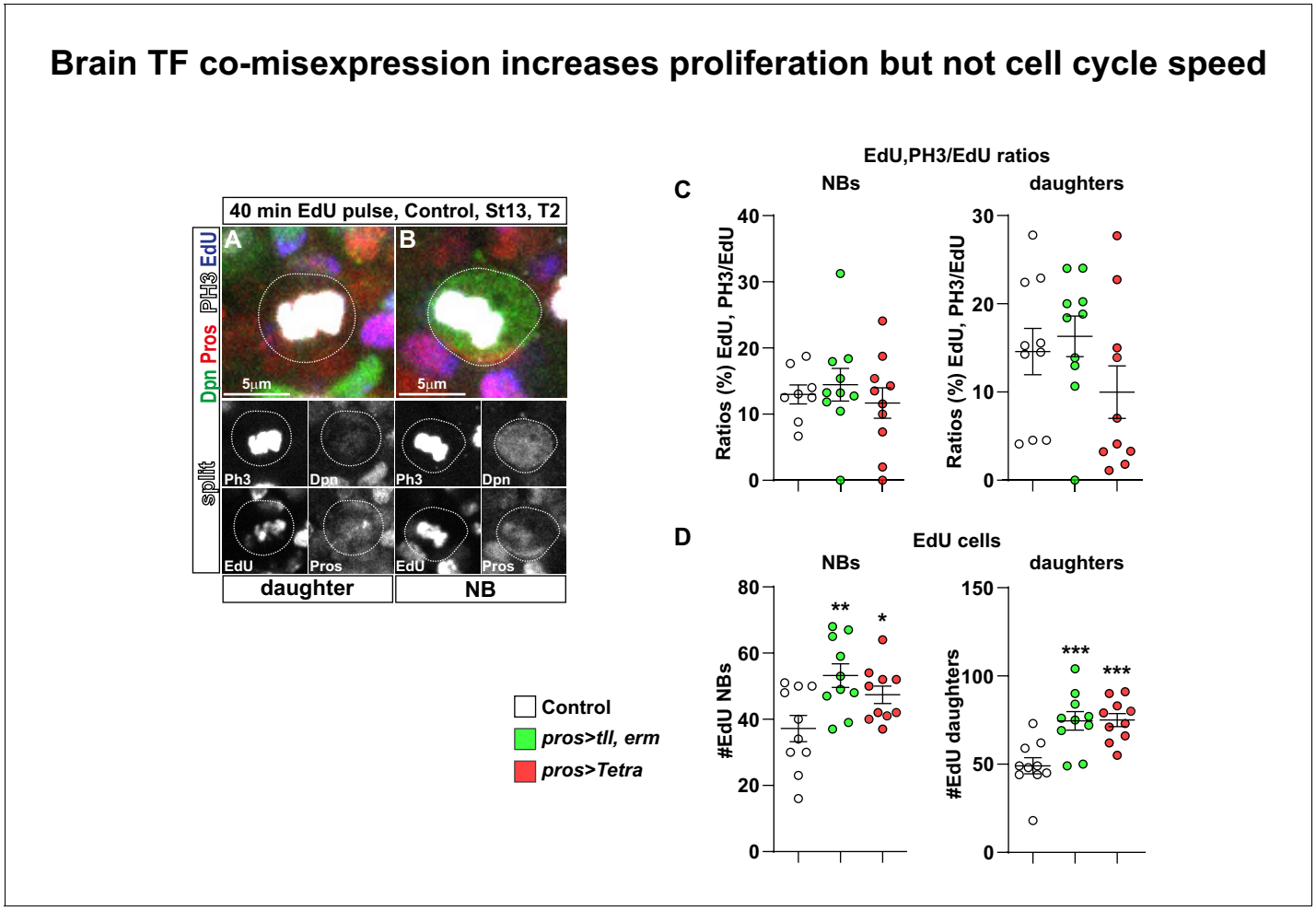

Figure 2—figure supplement 3. Brain TF co-misexpression increases EdU labelling but not cell cycle speed. (**A-B**) EdU labelled mitotic NBs or daughter cells, identified by expression of PH3, Dpn and Pros, following a 40 min EdU pulse at St13. (**C**) Quantitation of ratios (in percentage) of EdU/PH3 double-labelled NBs or daughter cells to total EdU single-labelled NBs or daughter cells, in control (*pros-Gal4/+*), *pros-Gal4 > UAS tll,-erm* and *pros-Gal4 > UAS* Tetra, T2 at St13 (Student's t test; mean ± SEM; n ≥ 10 embryos per genotype). (**D**) Quantitation of total EdU labelled NBs or daughter cells in the same three genotypes, T2 at St13 (Student's t test; $*p \leq 0.05$, $**p \leq 0.01$, $***p \leq 0.001$; mean ± SEM; n ≥ 10 embryos per genotype). Confocal images single optical sections.

DOI: https://doi.org/10.7554/eLife.45274.008

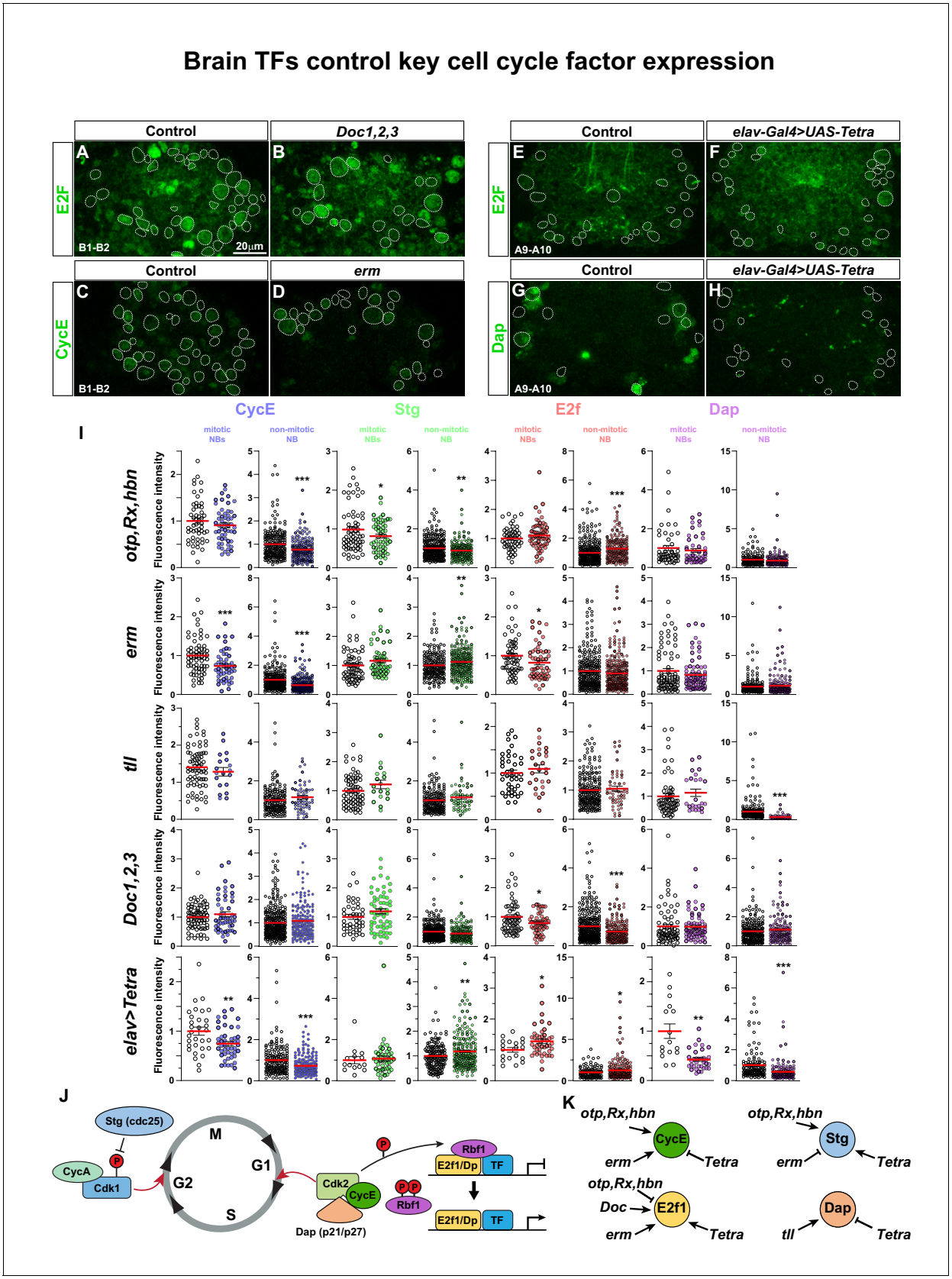

Figure 2—figure supplement 4. Brain TFs control key cell cycle factor expression. (**A-H**) Control (*OrR*), mutant or *elav-Gal4 > UAS* Tetra brain lobes or A9-A10 nerve cord segments, showing expression of E2F, CycE or Dap. Labelling for PH3, Pros and Dpn (not shown) allows for recognition of mitotic

Figure 2—figure supplement 4 continued on next page

Figure 2—figure supplement 4 continued

NBs (dashed circles). (**I**) Quantification of expression levels of the cell cycle factors CycE, Stg, E2f and Dap, in mitotic and non-mitotic NBs (Student's t test; $*p \leq 0.05$, $**p \leq 0.01$, $***p \leq 0.001$; mean ± SEM; $n \geq 3$ embryos, $n \geq 51$ NBs). (**J**) Cartoon depicting the main cell cycle role of the cell cycle factors analysed. (**K**) Model summarising the significant effects observed. Confocal images are single optical sections.

DOI: https://doi.org/10.7554/eLife.45274.009

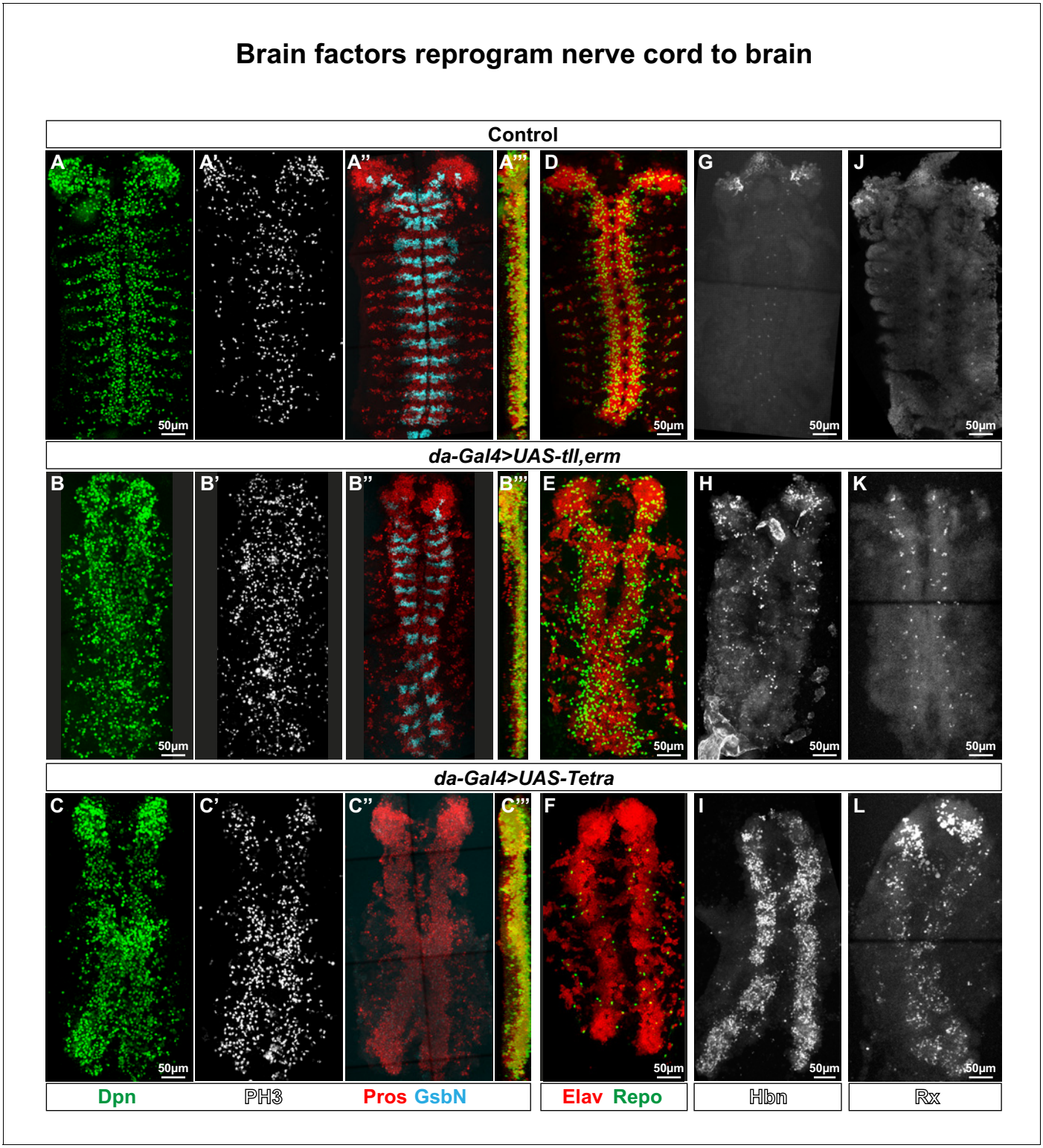

Figure 3. Brain TFs reprogram the nerve cord to a brain-like CNS. (**A-L**) Control (*da-Gal4/+*) and *da-Gal4/UAS-* co-misexpression embryo fillets, at St15, immunostained for Dpn, PH3, Pros, GsbN, Elav, Repo, Hbn or Rx. (A'''), (B''') and (C''') represent orthogonal projections of all four channels. (A-C''') *da-Gal4 > UAS tll,-erm* and *da-Gal4/UAS-Tetra* both result in generation of aberrant NBs (Dpn+), daughter cells (Pros+) and mitotic cells (PH3+). Expression of the segment polarity marker GsbN appears largely unaffected in *UAS-tll,-erm*, while *UAS-Tetra* results in widespread repression of GsbN expression in the nerve cord. (**D-E**) Co-misexpression of *tll,erm* triggers supernumerary neurons (Elav+) and glial cells (Repo+), while *Tetra* primarily

Figure 3 continued on next page

Figure 3 continued

generates extra neurons. (**G-L**) *da-Gal4 > UAS tll,-erm* and *da-Gal4/UAS-Tetra* both result in ectopic Hbn and Rx expression in the nerve cord, with *UAS-Tetra* showing the strongest effects. All confocal images are maximum intensity projections of multiple focal planes.

DOI: https://doi.org/10.7554/eLife.45274.011

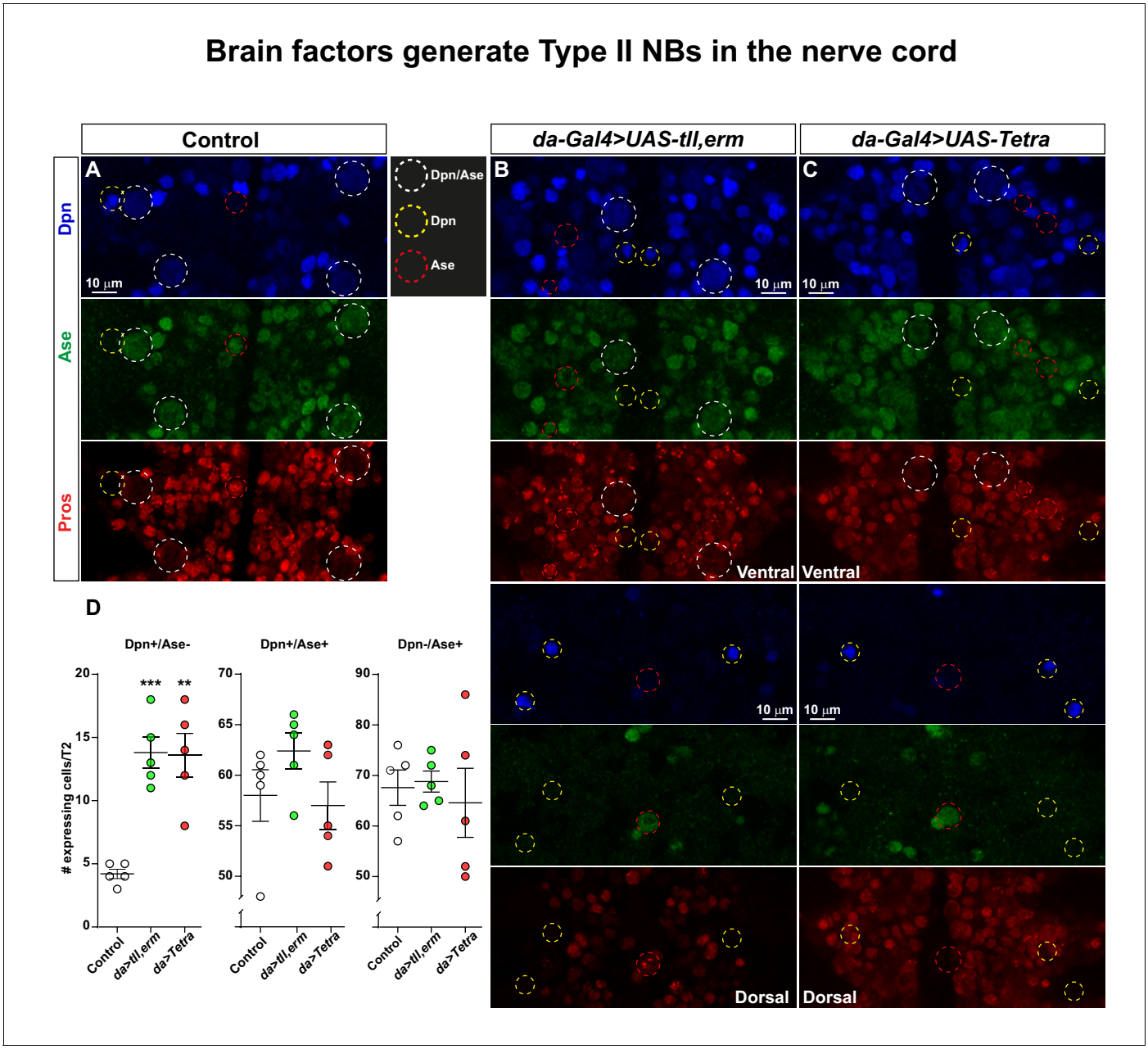

Figure 4. Brain TFs trigger generation of Type II-like NBs in the nerve cord. (**A-C**) Control (*da-Gal4/+*) and *da-Gal4/UAS-* co-misexpression embryo fillets, at St13, stained for Dpn, Ase and Pros. (**D**) Quantification of Dpn-only, Dpn/Ase and Ase-only expressing cells in control and misexpression, revealing significant increase in Dpn-only NBs in the co-misexpression embryos (Student's t test; $^{**}p \leq 0.01$, $^{***}p \leq 0.001$; mean ± SEM; $n \geq 5$ embryos). Confocal images are maximum intensity projections of multiple focal planes. Zoomed in images are single optical sections.

DOI: https://doi.org/10.7554/eLife.45274.012

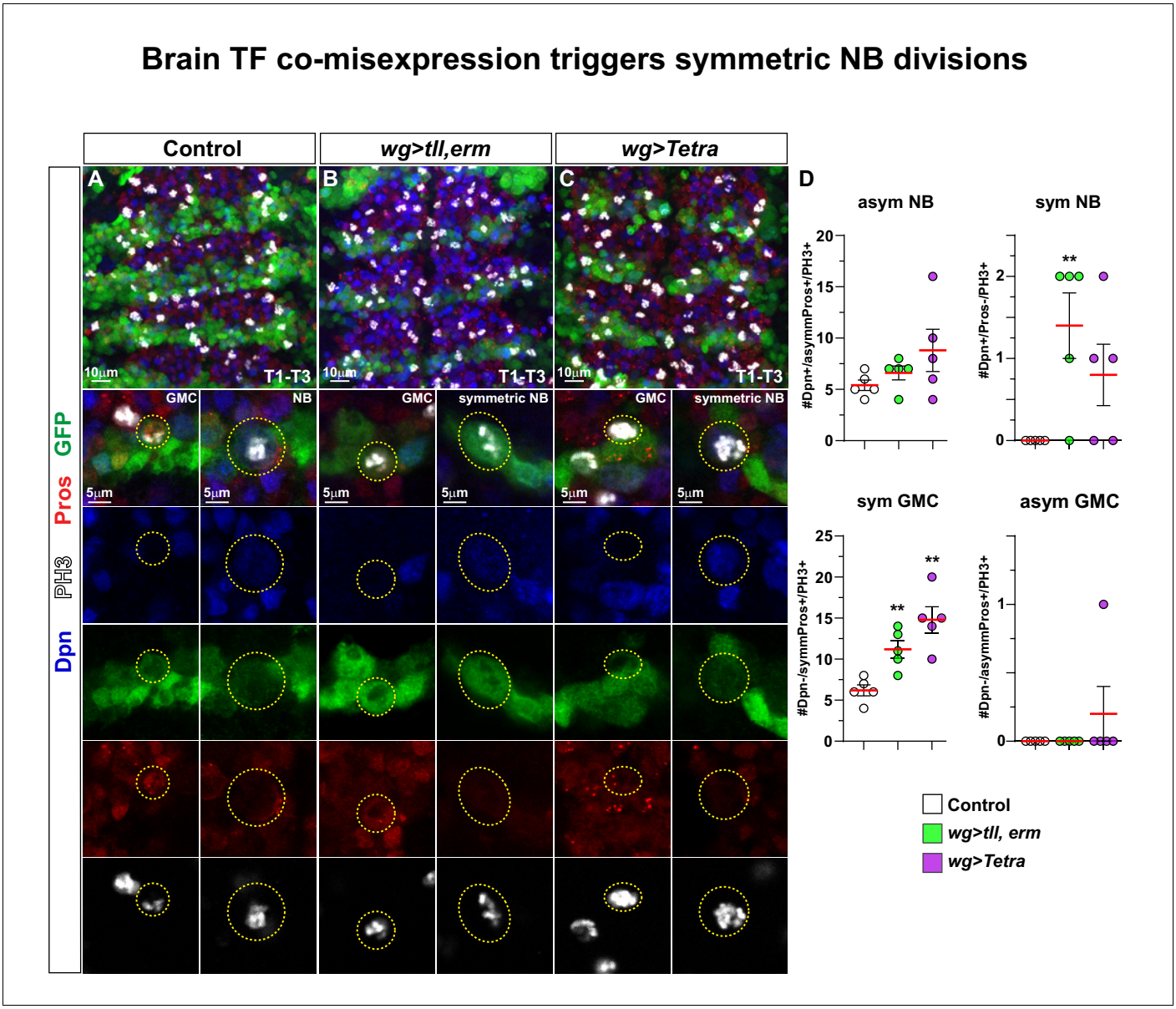

Figure 4—figure supplement 1. Brain TFs trigger symmetric NB divisions. (**A**) Control (*wg-Gal4/+*), St13 T1-T3, embryonic nerve cords display typical asymmetrically dividing NBs, and symmetrically dividing daughter cells (GMCs). (**B-C**) *wg-Gal4 > UAS tll,-erm* or *UAS-Tetra* triggers symmetric NB divisions. (**D**) Quantitation of the number of symmetrically and asymmetrically dividing NBs and GMCs. *tll,erm* co-misexpression triggers a significant increase in symmetrically dividing NBs, while *Tetra* shows an upward trend (Student's t test; mean ± SEM; $^{**}p \leq 0.01$; $n \geq 5$ embryos, $n \geq 15$ segments).
DOI: https://doi.org/10.7554/eLife.45274.013

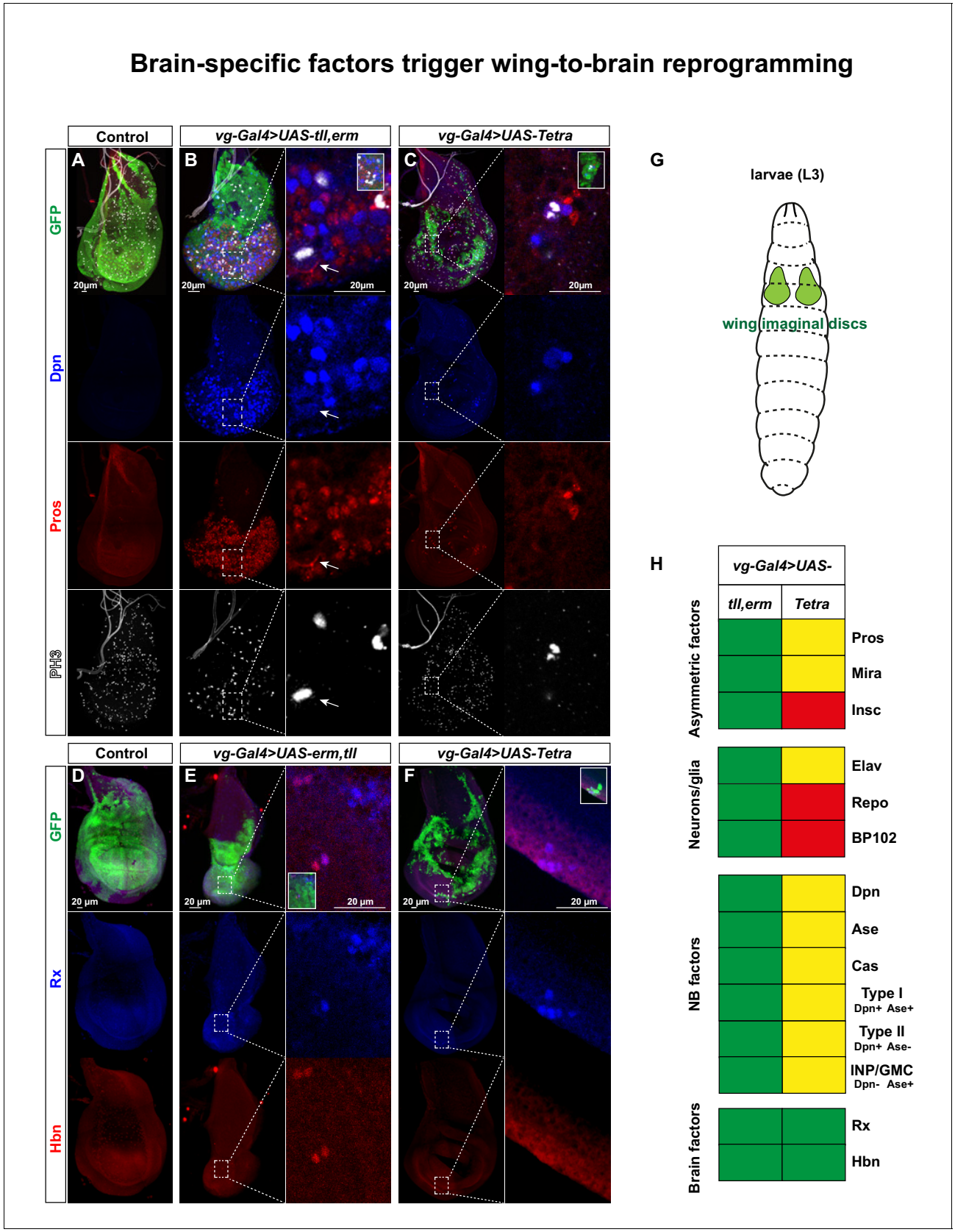

Figure 5. Brain TFs trigger wing-to-brain reprogramming. (**A**) Control (*vg-Gal4, UAS-GFP/+*) L3 larval imaginal wing discs do not display NBs, evident by lack of Dpn and Pros expressing cells. (**B-C**) *vg-Gal4, UAS-GFP > UAS tll, erm* or *UAS-Tetra* triggers ectopic NBs and daughter cell specification

Figure 5 continued on next page

Figure 5 continued

(arrow in B point to an asymmetrically dividing NB). (**D**) Control wing discs do not display expression of the brain markers Rx and Hbn. (**E-F**) *vg-Gal4, UAS-GFP > UAS tll,-erm* or *UAS-Tetra* triggers ectopic expression of Rx and Hbn. (**G**) Cartoon showing the developing wing imaginal discs in the L3 larvae. (**H**) Summary of the co-misexpression effects, based upon this figure, as well as figures S7-S10. In contrast to the embryonic misexpression effects (***Figures 2*** and ***3***), in the wing imaginal disc *tll,erm* shows a more complete NB reprogramming effect that *Tetra* (green = strong effect; yellow = intermediate effect; red = no effect; Pros is expressed in both *UAS* combinations, but only asymmetric in *tll,erm*). Confocal images of entire wing discs are maximum intensity projections of multiple focal planes. Zoomed in images are single optical sections.

DOI: https://doi.org/10.7554/eLife.45274.014

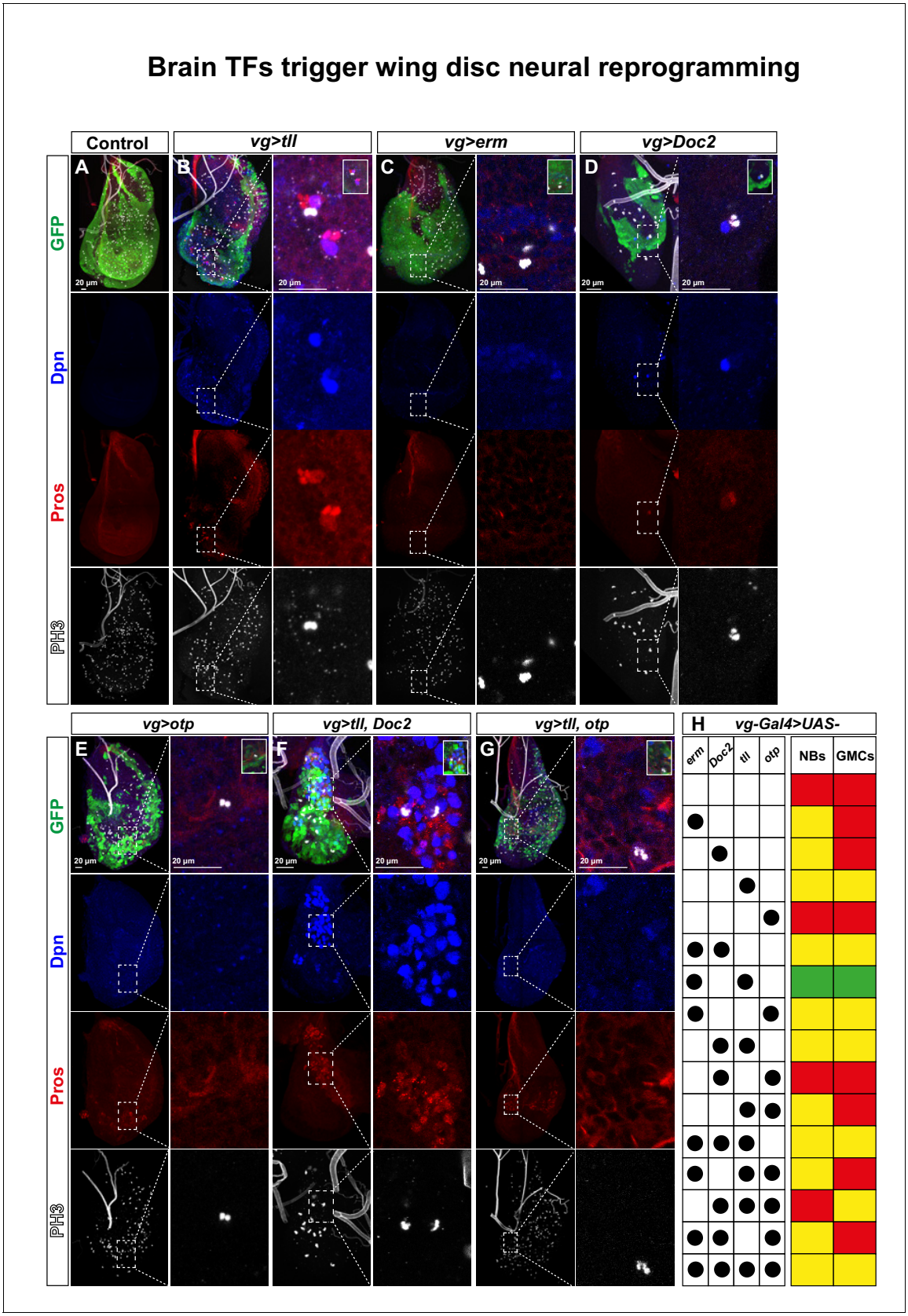

Figure 5—figure supplement 1. Brain TFs trigger wing disc neural reprogramming. (**A**) Control (*vg-Gal4/+*) L3 larval imaginal wing discs do not display NBs, evident by lack of expression of Dpn and Pros. (**B-G**) Single or double misexpression, driven by *vg-Gal4*, triggers varying degree of ectopic NB

Figure 5—figure supplement 1 continued on next page

Figure 5—figure supplement 1 continued

generation, evident by Dpn and Pros expression. (**H**) Summary of all 15 single, double, triple and tetra misexpression effects observed in the wing discs (green = strong effect; yellow = intermediate effect; red = no effect). Note that control images in A are reproduced for reference in S8A. Confocal images of entire wing discs are maximum intensity projections of multiple focal planes. Zoomed in images are single optical sections.

DOI: https://doi.org/10.7554/eLife.45274.015

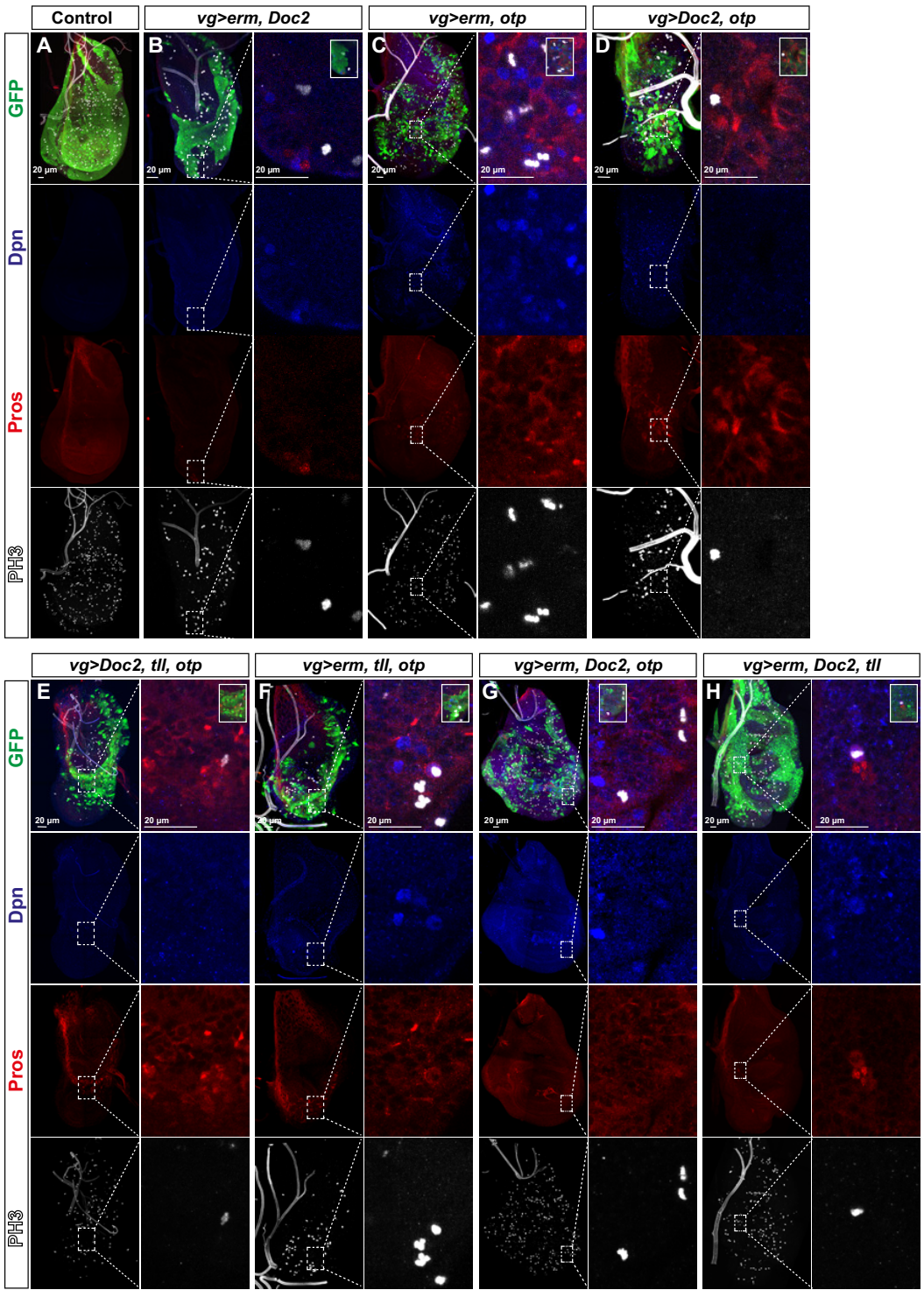

Figure 5—figure supplement 2. Brain TFs trigger wing disc neural reprogramming. (**A**) Control (*vg-Gal4/+*) L3 larval imaginal wing discs do not display NBs, evident by lack of expression of Dpn and Pros (note that these control images are reproduced from ***Figure 5—figure supplement 1***). (**B-H**)

Figure 5—figure supplement 2 continued on next page

Figure 5—figure supplement 2 continued

Double or triple misexpression, driven by *vg-Gal4*, triggers varying degree of ectopic NB generation, evident by Dpn and Pros expression. Confocal images of entire wing discs are maximum intensity projections of multiple focal planes. Zoomed in images are single optical sections.

DOI: https://doi.org/10.7554/eLife.45274.016

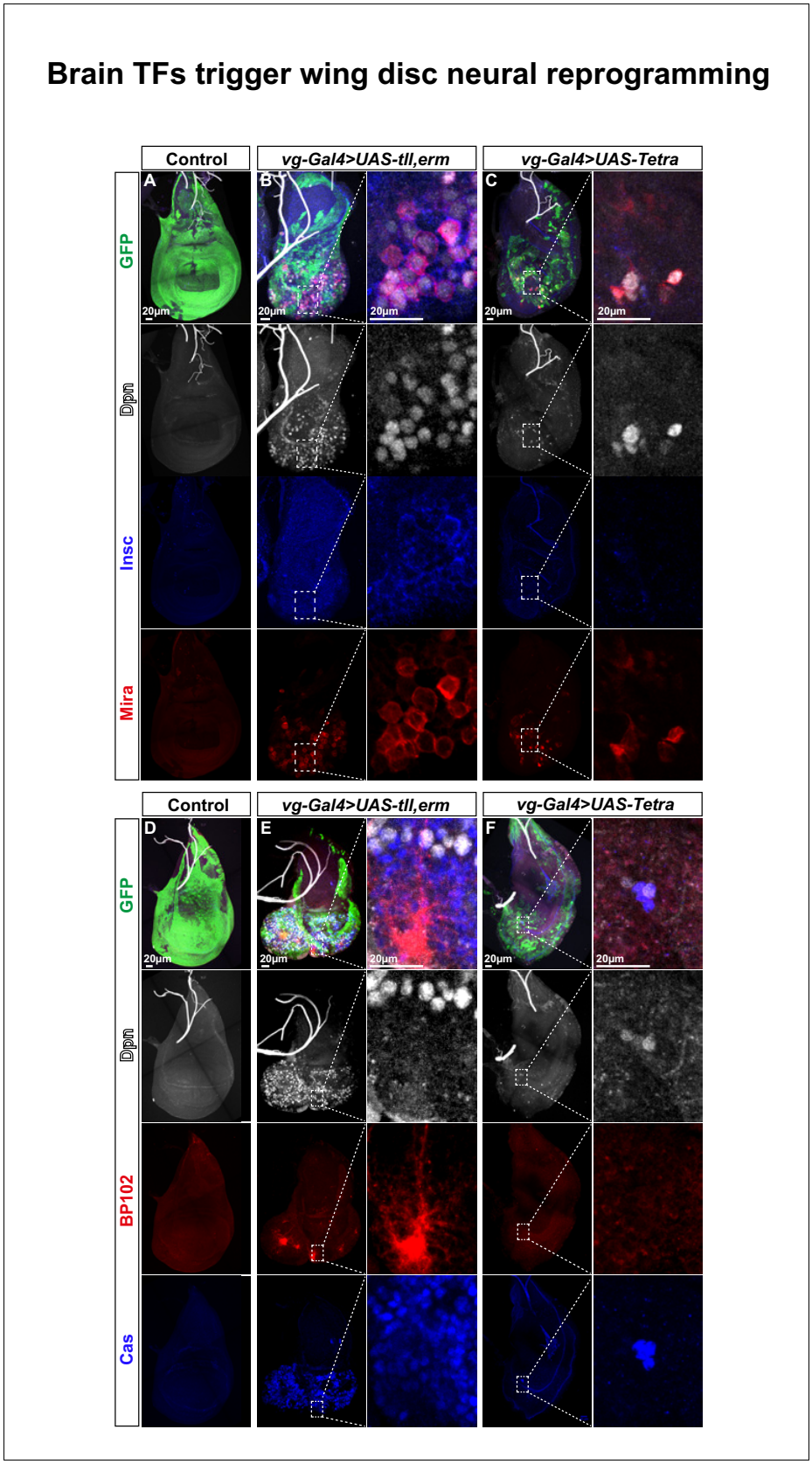

Figure 5—figure supplement 3. Brain TFs trigger wing disc neural reprogramming. (**A**) Control (*vg-Gal4/+*) L3 larval imaginal wing discs do not display NBs, evident by lack of expression of Dpn and of the asymmetric cell

Figure 5—figure supplement 3 continued on next page

Figure 5—figure supplement 3 continued

division NB markers Insc and Mira. (**B-C**) *vg-Gal4 > UAS tll,-erm* triggers generation of ectopic NBs, with ectopic expression of both Insc and Mira, while *UAS-Tetra* generates few NBs and only triggers Mira expression. (**D**) Control imaginal discs do not display NBs (Dpn) or expression of the interneuron markers BP102 or of the late temporal NB factor Cas. (**E-F**) *vg-Gal4 > UAS tll,-erm* triggers ectopic expression of Dpn, BP1023 and Cas, while *UAS-Tetra* only triggers minimal activation of Cas. Confocal images of entire wing discs are maximum intensity projections of multiple focal planes. Zoomed in images are single optical sections.

DOI: https://doi.org/10.7554/eLife.45274.017

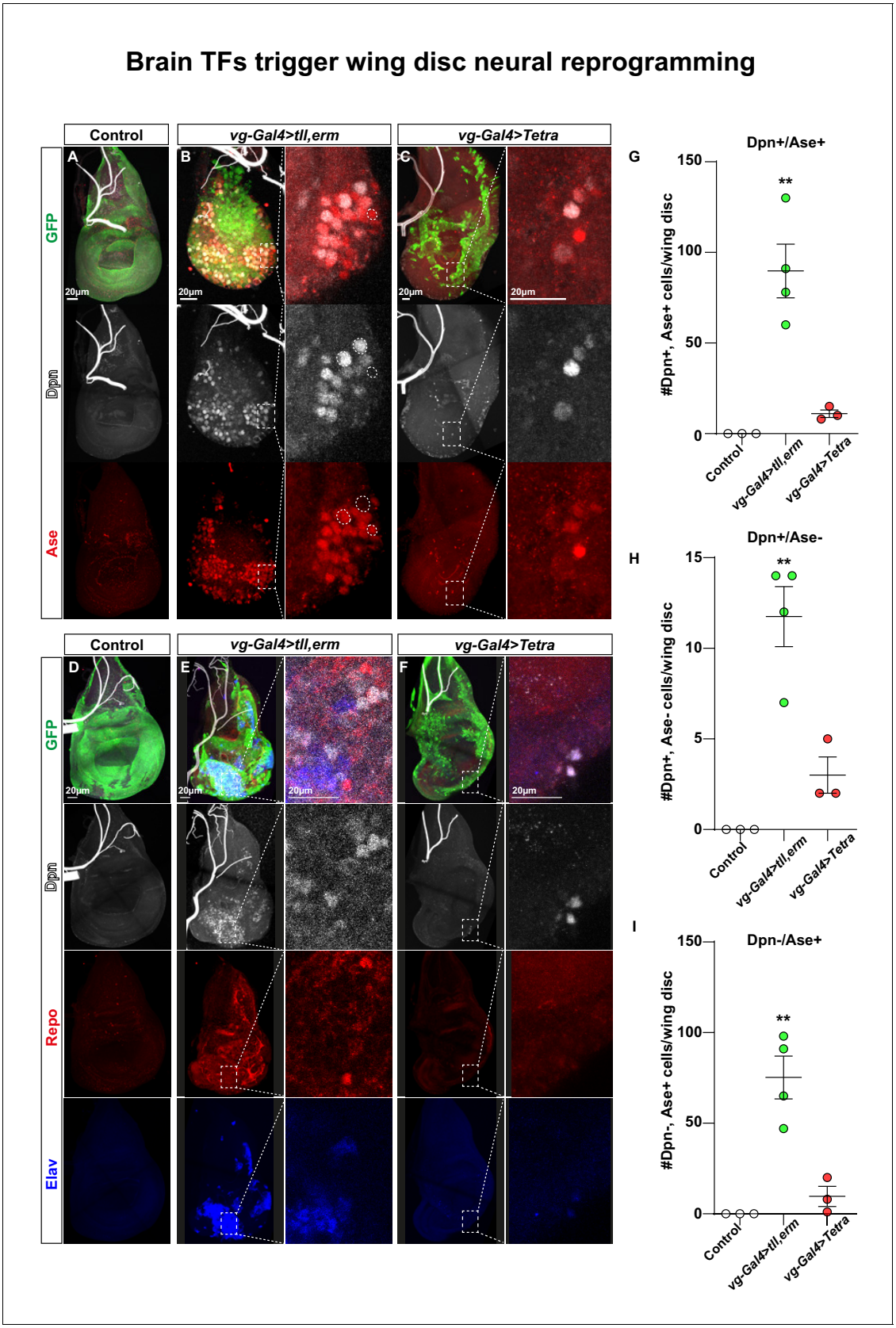

Figure 5—figure supplement 4. Brain TFs trigger wing disc neural reprogramming. (**A**) Control (*vg-Gal4/+*) L3 larval imaginal wing discs do not display NBs, evident by lack of expression of Dpn and of the NB marker Ase. (**B-C**) *vg-Gal4 > UAS tll,-erm* or *UAS-Tetra* triggers the generation of ectopic NBs,

Figure 5—figure supplement 4 continued on next page

Figure 5—figure supplement 4 continued

with Ase expression. (**D**) Control imaginal discs do not display NBs (Dpn), or expression of the neuron marker Elav or the glia marker Repo. (**E-F**) *vg-Gal4 > UAS tll,-erm* triggers robust ectopic expression of Dpn, Elav and Repo, while *UAS-Tetra* has weaker much effects. (**G-I**) Quantification of the number of Type I-like NBs (Dpn+/Ase+), Type II-like NBs (Dpn+/Ase-) and INP/GMC-like cells (Dpn-/Ase+) in the wing disc, measured in a 2387 µm2 area of the wing pouch (Student's t test; $^{**}p \leq 0.01$; mean ± SEM; $n \geq 3$ wing discs). Confocal images of entire wing discs are maximum intensity projections of multiple focal planes. Zoomed in images are single optical sections.

DOI: https://doi.org/10.7554/eLife.45274.018

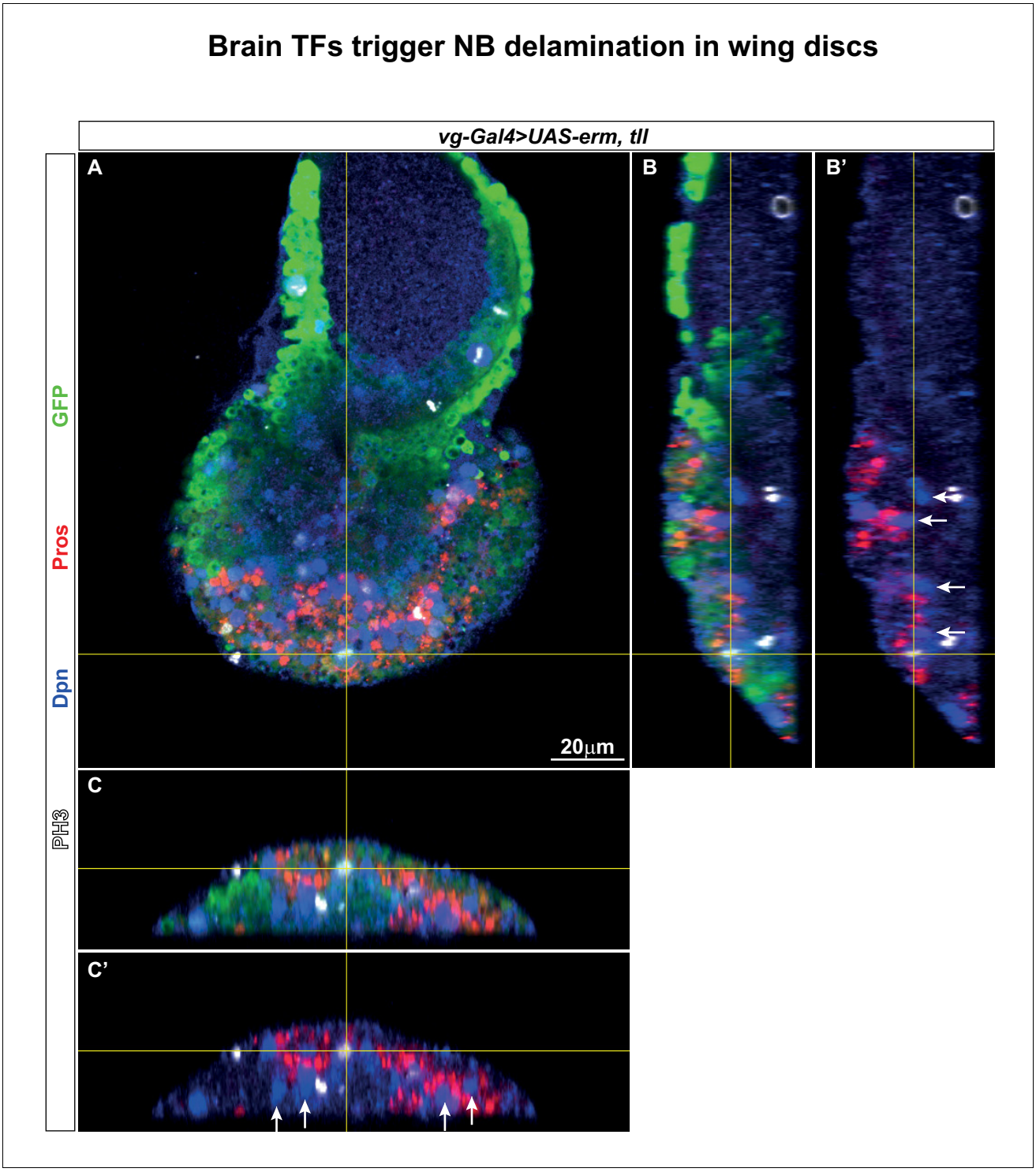

Figure 5—figure supplement 5. Brain TFs trigger NB delamination in wing discs. (**A-C'**) *vg-Gal4 > UAS tll,-erm* L3 larval imaginal wing discs display generation of ectopic NBs, evident by Pros and Dpn expression. (**B-C'**) Orthogonal optical cross-sections reveal that wing disc cells that are reprogrammed to NBs often delaminate from the epithelial plane (arrows). Confocal images of entire wing discs are maximum intensity projections of multiple focal planes.

DOI: https://doi.org/10.7554/eLife.45274.019

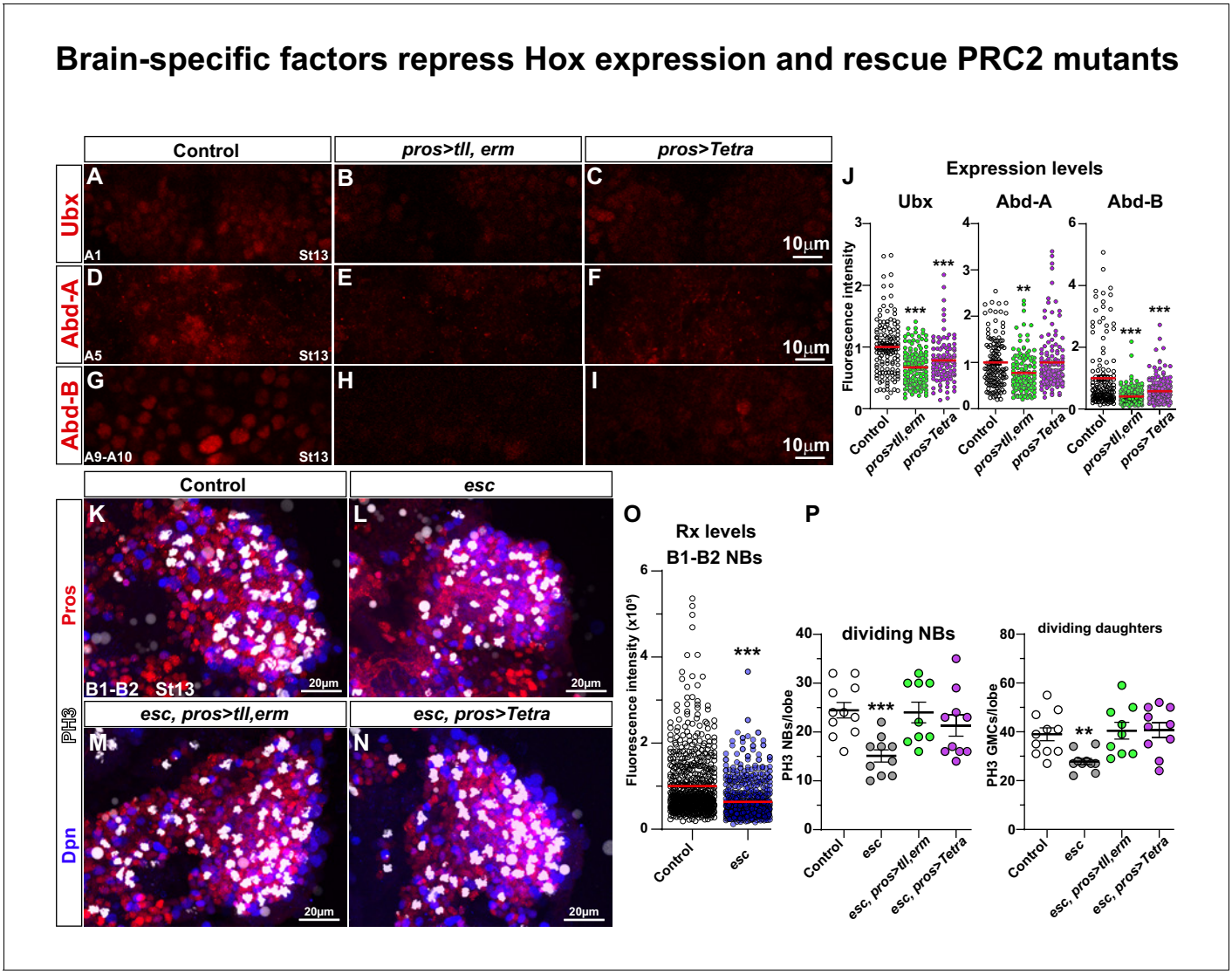

Figure 6. Brain TFs repress Hox expression and rescue PRC2 mutants. (**A-I**) Control (*da-Gal4/+)* and *da-Gal4/UAS-* co-misexpression embryo nerve cords, at St13, stained for Ubx, Abd-A or Abd-B, in the highest-expressing abdominal segment for each Hox factor (A1 for Ubx; A5 for Abd-A; A8-A10 for Abd-B) (***Monedero Cobeta et al., 2017***). (**J**) Quantification of Ubx, Abd-A and Abd-B expression levels in NBs in the same respective segments (Student's t test; $^{**}p\leq0.01$, $^{***}p\leq0.001$; mean ± SEM; n ≥ 3 embryos, n ≥ 108 NBs). (**K-N**) Control (*OrR*), *esc* maternal/zygotic mutants, and *esc* maternal/zygotic mutants co-expressing *tll,erm* (*pros > tll, erm*) or *Tetra* (*pros > Tetra*), stained for Dpn, Pros and PH3. In *esc* maternal/zygotic mutants, proliferation is reduced. This phenotype can be rescued by either *UAS-tll,-erm* or *UAS-Tetra* expression. (**O**) Quantification of Rx expression in B1-B2 NBs, in control and *esc* mutants, reveal significant reduction of Rx in *esc* mutants (Mann-Whitney U-test; $^{***}p\leq0.001$; mean ± SD; n ≥ 6 brain lobes, n ≥ 620 NBs per genotype). (**P**) Quantitation of NB and daughter cell proliferation (Student's t test; $^{**}p\leq0.01$, $^{***}p\leq0.001$; mean ± SD; n ≥ 9 embryos per genotype; note that control data in P are reproduced for reference from ***Figure 1G–H***). (**A-I**) Single optical sections. (**K-N**) Maximum intensity projections of multiple focal planes.

DOI: https://doi.org/10.7554/eLife.45274.020

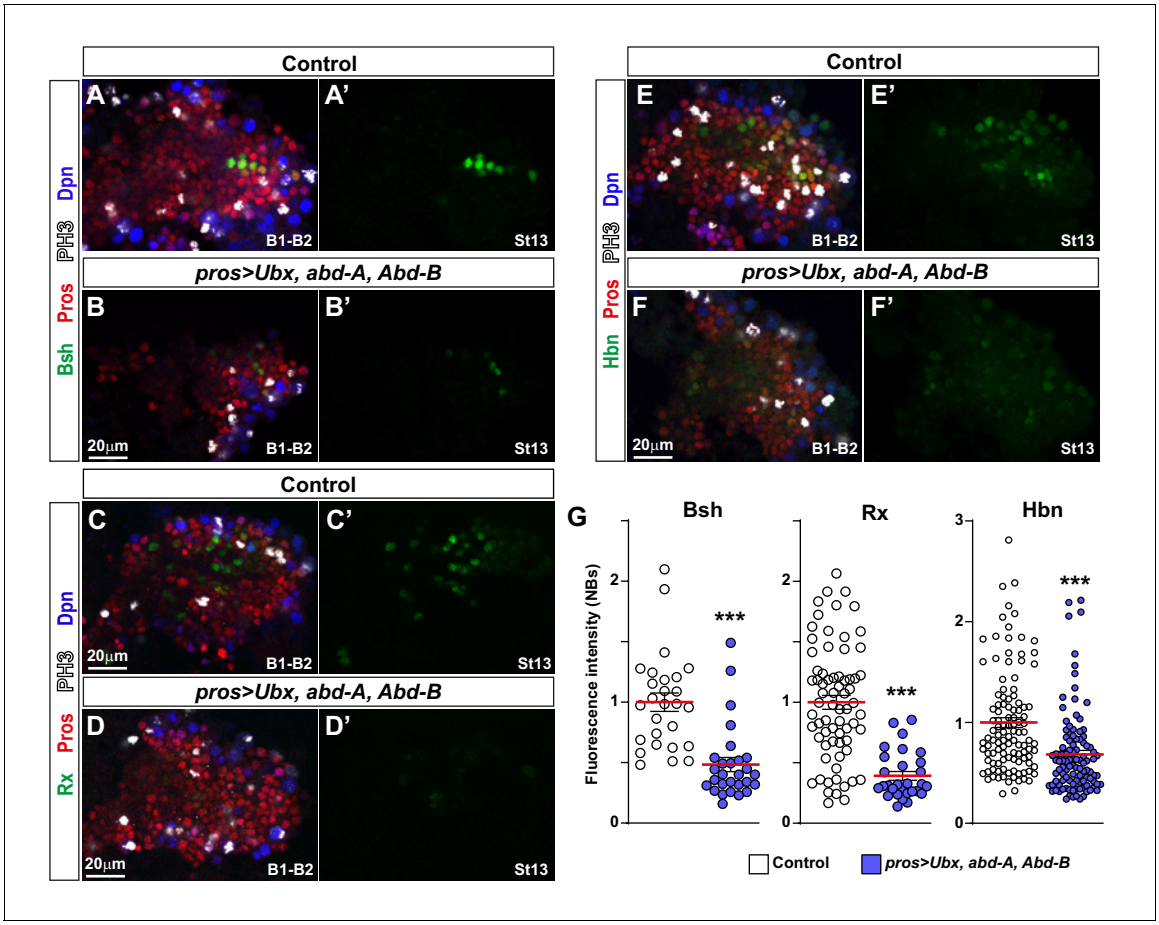

Figure 6—figure supplement 1. Hox genes repress brain TFs. (**A-F'**) Control (*pros-Gal4/+*) and *pros-Gal4/UAS-Ubx,-abd-A,-Abd-B* co-misexpressing brain lobes, showing expression of the brain factors Bsh, Rx and Hbn, at St13. Bsh, Rx and Hbn expression is reduced by triple Hox co-misexpression. (**G**) Quantitation of Bsh, Rx and Hbn expression levels in brain lobe NBs (Student's t test; ***$p \leq 0.001$; mean ± SD; $n \geq 3$ embryos and $n \geq 27$ NBs per genotype). Confocal images are single optical sections.

DOI: https://doi.org/10.7554/eLife.45274.021

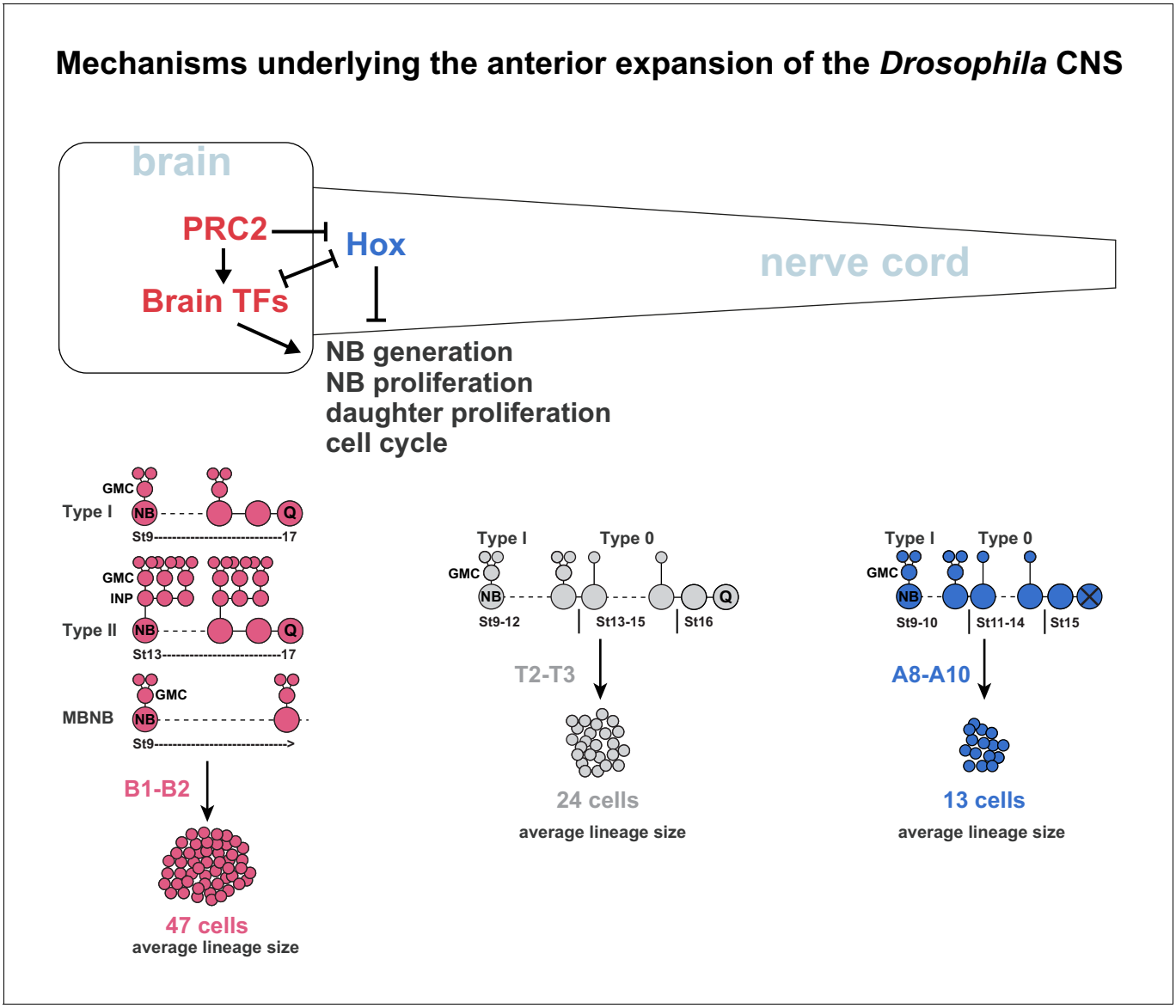

Figure 7. Mechanisms underlying the anterior expansion of the *Drosophila* CNS. Brain TFs act in two manners to promote anterior CNS expansion. First, brain TFs drive the super-generation of NBs observed in the B1 brain segment. Second, brain TFs promote the three different hyper-proliferative lineage progression modes observed in the brain; Type I, Type II and MBNB, which manifest as an extended phase of NB proliferation and more elaborate daughter cell proliferation. In the nerve cord, Hox genes act to limit NB and daughter cell proliferation, resulting in a switch from Type I to Type 0 proliferation, and an earlier NB cell cycle exit. The distinct lineage profiles evident in the brain versus nerve cord result in dramatically different average lineages sizes along the A-P axis. The combination of NB super-generation and the hyper-proliferative lineage modes results in vastly more cells generated in the brain B1 segments than in the nerve cord segments (***Monedero Cobeta et al., 2017***; ***Yaghmaeian Salmani et al., 2018***). PRC2 acts to prevent Hox gene expression in the brain, thereby promoting brain TF expression and thereby anterior CNS expansion.

DOI: https://doi.org/10.7554/eLife.45274.022